Numerical solution of stiff parabolic differential equations describing gas fluidized beds with a two-phase model

Please check the document version of this publication:

NUMERICAL SOLUTION OF STIFF PARABOLIC DIFFERENTIAL EQUATIONS DESCRIBING GAS FLUIDIZED BEDS WITH A TWO-PHASE MODEL

C. E. J. VAN LARE, H. W. PIEPERS[†] and D. THOENES

Eindhoven University of Technology, Department of Chemical Engineering, Laboratory of Chemical Process Technology, PO Box 513, 5600 MB, Eindhoven, Netherlands

Abstract—A model for the non-steady-state description of gas fluidized beds is derived, based on the bubble dispersion model. For the solution of the (parabolic) differential equations describing the non-steady- and steady-state situations, a new method is used: the decoupling method. It is mathematically and numerically not complex and good results are obtained.

INTRODUCTION

Residence time distribution (RTD) measurement is a strong and (experimentally) relatively simple method in determining physical parameters, such as mass transfer or mixing coefficients. Therefore, the RTD curve has to be measured experimentally and fitted numerically. In principle, this method can also be applied to chemical reacting systems. For example, in gas fluidized beds, information can then be subtracted from the start up period, combined with the steady-state and/or shut down period. In both cases the system in consideration must be described mathematically. It is not unlikely one obtains a system of equations that is not solvable analytically and sometimes even not numerically.

The numerical methods that are used most for non-steady-state problems are the Crank–Nicholson technique [for instance Eigenberger and Butt (1976)] and orthogonal collocation (Villadsen and Stewart, 1967). Both methods can lead to erroneous answers and/or excessive calculation time for stiff problems (Hlavacek and van Rompay, 1981).

Van Loon (1987) obtained good results for steady-state stiff boundary value problems using the decoupling method. We examined whether this approach could be employed for non-steady-state equations. It could then be used for a sensitivity analysis.

A numerical method is described for solving a set of (stiff) parabolic differential equations describing the non-steady-state behavior of gas fluidized beds. This method decouples the equations into a "decoupled space". There the solution is calculated and by back transformation the final solution is obtained (analogous to Laplace transformation).

MODEL DESCRIPTION

Several models have been proposed for describing gas fluidized beds. The van Deemter (1961) model and the bubble dispersion model [for instance Dry and

Judd (1985)] give a good insight into mass transfer and mixing. Both are simple physical descriptions of a gas fluidized bed with just a few (unknown) fitted parameters. Results when using this model have been good [see, for instance, van Swaaij and Zuiderweg (1972), Werther (1978), Bauer (1980), Dry and Judd (1985) and van Lare *et al.* (1990)]. They are mostly used for describing the behavior of A- or B-type powders, according to the Geldart (1973) classification. We describe both the bubble and the dense phase as plug flow reactors with axial dispersion, and allow mass transfer between both phases (Fig. 1).

Here we have the superficial velocity U with regard to the cross-sectional area A of the reactor. The gas flows through the dense phase with a volumetric flow rate of $\varphi U_{mf} A$. The factor φ accounts for the fact that more gas can flow through the dense phase than is described by the two-phase theory (where $\varphi = 1$). Especially for D-type powders, values of φ greater than 1 are important because of the relatively small $U/(\varphi U_{mf})$ values. Even for A-type powders several values of φ are reported (Grace and Clift, 1974). However these deviations are not that important because of the large $U/(\varphi U_{mf})$ values.

Furthermore, we define a mass transfer coefficient K_e (that can be regarded as $k_g a$) and Eddy dispersion coefficients for the bubble phase (E_b) and dense phase (E_d). The bubble hold up δ, the dense-phase porosity ε_d, φ, K_e, E_b and E_d are taken to be independent of the height h, implying that height-averaged values are used. By definition reaction can only take place in the dense phase, because there are no (catalyst) particles in the bubble phase. A rate constant k_m is defined, based on catalyst mass. We consider a first-order reaction.

Taking a mass balance over a slice dh leads to

$$\delta \frac{\partial C_b}{\partial t} = -(U - \varphi U_{mf}) \frac{\partial C_b}{\partial h}$$

$$- K_e(C_b - C_d) + E_b \delta \frac{\partial^2 C}{\partial h^2} \quad (1a)$$

[†]Author to whom correspondence should be addressed.

$$C_{out} = f_b \cdot C_{b,H} + (1 - f_b) \cdot C_{d,H}$$

$$(U - \varphi \cdot U_{mf}) C_{b,h+dh} \qquad\qquad \varphi \cdot U_{mf} \cdot C_{d,h+dh}$$

$$-E_b \delta \left[\frac{dC_b}{dh}\right]_{h+dh} \qquad\qquad -E_d(1-\delta)\varepsilon_d \left[\frac{dC_d}{dh}\right]_{h+dh}$$

$$K_e$$

$$-E_b \delta \left[\frac{dC_b}{dh}\right]_{h} \qquad\qquad -E_d(1-\delta)\varepsilon_d \left[\frac{dC_d}{dh}\right]_{h}$$

$$(U - \varphi \cdot U_{mf}) C_{b,h} \qquad\qquad \varphi \cdot U_{mf} \cdot C_{d,h}$$
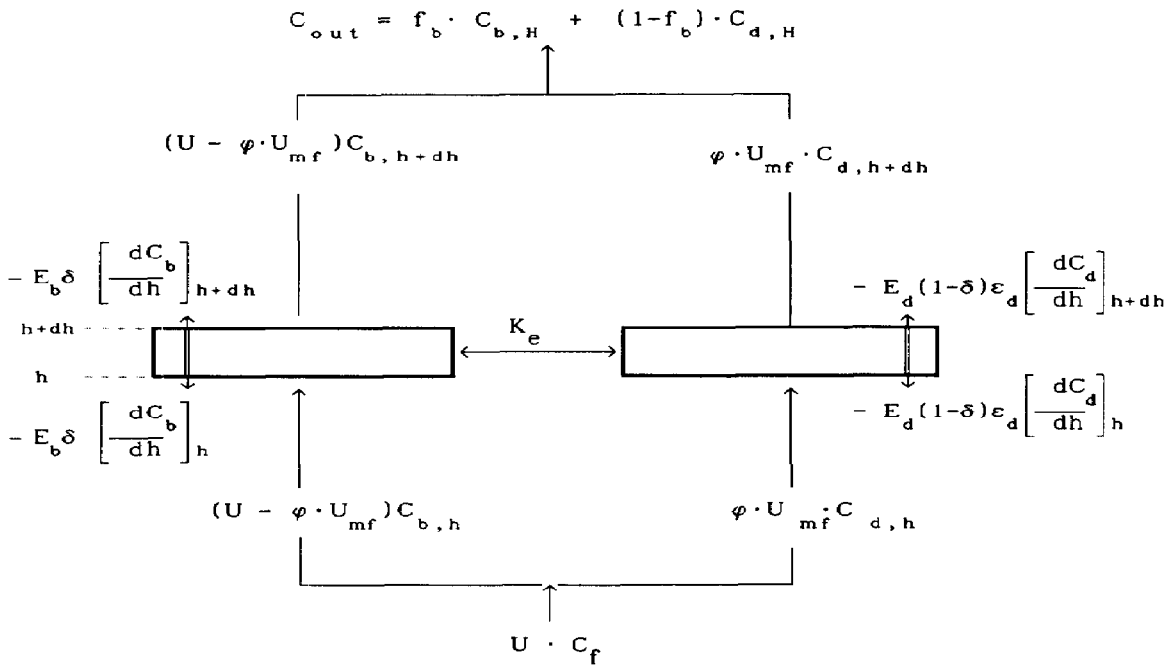
$$U \cdot C_f$$

Fig. 1. Schematic presentation of flow division in a gas fluidized bed.

$$(1 - \delta)\varepsilon_d \frac{\partial C_d}{\partial t} = -\varphi U_{mf} \frac{\partial C_d}{\partial h} - K_e(C_d - C_b)$$

$$+ E_d(1 - \delta)\varepsilon_d \frac{\partial^2 C_d}{\partial h^2} - k_m(1 - \delta)(1 - \varepsilon_d)\rho_p C_d \quad \text{(1b)}$$

with boundary conditions:

for $t \le 0$ there is no (tracer) gas in the reactor:

$$C_b(0, h) = 0 \tag{2a}$$

$$C_d(0, h) = 0 \tag{2b}$$

injection at distributor ($h = 0$) and backmixing from column:

$$C_b(t, 0) = C_f(t) + \frac{1}{f_b \cdot Pe_b} \frac{\partial C_b}{\partial h}\bigg]_{h=0} \qquad (t > 0) \tag{2c}$$

$$C_d(t, 0) = C_f(t) + \frac{1}{(1 - f_b) \cdot Pe_d} \frac{\partial C_d}{\partial h}\bigg]_{h=0} \qquad (t > 0)$$

$$\tag{2d}$$

no concentration gradient at fluid bed surface:

$$\frac{\partial C_b}{\partial h}\bigg]_{h=H} = 0 \tag{2e}$$

$$\frac{\partial C_d}{\partial h}\bigg]_{h=H} = 0. \tag{2f}$$

We define an average residence time τ based on the total fraction of gas in the reactor and not only on the fraction of gas in the bubble phase. For A/B-type powders the difference is very small. However, for D-type powders it is essential to take the fraction of gas

in the dense phase into account. Furthermore, we define an average residence time for the bubble phase (τ_b) and for the dense phase (τ_d):

$$\tau_b = \frac{H}{u_b} = \frac{H\delta}{U - \varphi U_{mf}}$$

(with u_b = bubble velocity) (3a)

$$\tau_d = \frac{H}{u_d} = \frac{H(1 - \delta)\varepsilon_d}{\varphi U_{mf}}$$

(with u_d = dense-phase gas velocity) (3b)

$$\tau = f_b \tau_b + (1 - f_b)\tau_d = \frac{H\xi}{U}, \text{ with } \xi = \delta + (1 - \delta)\varepsilon_d$$

and

$$f_b = (U - \varphi U_{mf})/U = \text{fraction of gas in}$$
$$\text{the bubble phase.} \quad (3c)$$

For A/B-type powders $f_b \simeq 1$, and therefore $\tau \simeq \tau_b$, which is a common assumption. Making eqs (1) and (2) dimensionless leads to

$$\frac{\partial C_b}{\partial \vartheta} + \beta \frac{\partial C_b}{\partial \sigma} + N_k \frac{\xi}{\delta}(C_b - C_d) - \frac{1}{Pe_b} \frac{\xi}{\delta} \frac{\partial^2 C_b}{\partial \sigma^2} = 0$$

$$\tag{4}$$

$$\frac{\partial C_d}{\partial \vartheta} + \gamma \frac{\partial C_d}{\partial \sigma} + \frac{N_k \xi}{(1 - \delta)\varepsilon_d}(C_d - C_b)$$

$$- \frac{1}{Pe_d} \frac{\xi}{(1 - \delta)\varepsilon_d} \frac{\partial^2 C_d}{\partial \sigma^2}$$

$$+ N_r \frac{\xi}{(1 - \delta)\varepsilon_d} C_d = 0 \tag{5}$$

with boundary conditions

$$C_b(0, \sigma) = 0 \qquad (6)$$

$$C_d(0, \sigma) = 0 \qquad (7)$$

$$C_b(\vartheta, 0) = C_f(\vartheta) + \frac{1}{f_b \cdot Pe_b} \frac{\partial C_b}{\partial \sigma}\bigg]_{\sigma = 0} \qquad (\vartheta > 0) \quad (8)$$

$$C_d(\vartheta, 0) = C_f(\vartheta) + \frac{1}{(1 - f_b) \cdot Pe_d} \frac{\partial C_d}{\partial \sigma}\bigg]_{\sigma = 0} \qquad (\vartheta > 0)$$
$$(9)$$

$$\frac{\partial C_b}{\partial \sigma}\bigg]_{\sigma = 1} = 0 \qquad (10)$$

$$\frac{d}{d\sigma} \begin{bmatrix} C_{b,i} \\ C_{d,i} \\ \partial C_{b,i}/\partial\sigma \\ \partial C_{d,i}/\partial\sigma \end{bmatrix} = \begin{bmatrix} 0 & 0 & 1 & 0 \\ 0 & 0 & 0 & 1 \\ Pe_b[N_k + \delta/(\xi \cdot \Delta\vartheta)] & -N_k \cdot Pe_b & f_b \cdot Pe_b & 0 \\ -N_k \cdot Pe_d & Pe_d[N_k + N_r + (1-\delta)\varepsilon_d/(\xi \cdot \Delta\vartheta)] & 0 & (1-f_b)Pe_d \end{bmatrix}$$

$$\times \begin{bmatrix} C_{b,i} \\ C_{d,i} \\ \partial C_{b,i}/\partial\sigma \\ \partial C_{d,i}/\partial\sigma \end{bmatrix} + \begin{bmatrix} 0 \\ 0 \\ -(Pe_b \cdot \delta/(\xi \cdot \Delta\vartheta))C_{b,i-1} \\ -\dfrac{Pe_d(1-\delta)\varepsilon_d}{\xi\Delta\vartheta} C_{d,i-1} \end{bmatrix}. \qquad (17)$$

$$\frac{\partial C_d}{\partial \sigma}\bigg]_{\sigma = 1} = 0. \qquad (11)$$

We use the following parameter definitions:

$$\beta = f_b \xi/\delta \qquad \vartheta = \frac{t}{\tau} \qquad \sigma = \frac{h}{H}$$

$$\gamma = \frac{(1 - f_b)\xi}{(1 - \delta)\varepsilon_d} \qquad N_k = \frac{K_e H}{U}$$

$$N_r = \frac{k_m(1 - \delta)(1 - \varepsilon_d)\rho_p H}{U} \qquad Pe_b = \frac{HU}{\delta E_b}$$

$$Pe_d = \frac{HU}{E_d(1 - \delta)\varepsilon_d}. \qquad (12)$$

If we assume that the bubble phase is in ideal plug flow ($E_b = 0$), we get the van Deemter (1961) model. If we neglect the dense-phase flow we get the well-known simplifications

$$f_b = 1 \quad \text{and} \quad \xi = \delta. \qquad (13)$$

In steady state ($\partial C/\partial\vartheta) = 0$), this leads to the modified van Deemter model (van Swaaij and Zuiderweg, 1972).

THE DECOUPLING METHOD

The Crank–Nicholson technique uses a finite difference in the space variable σ. We, however, use an Euler approximation for the time variable ϑ:

$$\frac{\partial C_x}{\partial\vartheta} \simeq \frac{C_{x,i} - C_{x,i-1}}{\vartheta_i - \vartheta_{i-1}} = \frac{C_{x,i} - C_{x,i-1}}{\Delta\vartheta},$$

$$\text{with } x = b, d. \qquad (14)$$

Substitution in eqs (4) and (5) leads to

$$\frac{\partial^2 C_{b,i}}{\partial\sigma^2} = f_b \cdot Pe_b \cdot \frac{\partial C_{b,i}}{\partial\sigma} + N_k \cdot Pe_b \cdot (C_{b,i} - C_{d,i})$$
$$+ \frac{C_{b,1} - C_{b,i-1}}{\Delta\vartheta} \frac{Pe_b \cdot \delta}{\xi} \qquad (15)$$

$$\frac{\partial^2 C_{d,i}}{\partial\sigma^2} = (1 - f_b) Pe_d \frac{\partial C_{d,i}}{\partial\sigma}$$
$$+ N_k \cdot Pe_d \cdot (C_{d,i} - C_{b,i}) + N_r \cdot Pe_d \cdot C_{d,i}$$
$$+ \frac{C_{d,i} - C_{d,i-1}}{\Delta\vartheta} \frac{Pe_d(1 - \delta)\varepsilon_d}{\xi}. \qquad (16)$$

Writing these equations in matrix form gives

In short:

$$\frac{d}{d\sigma} \mathbf{X}^i(\sigma) = \mathbf{A} \cdot \mathbf{X}^i(\sigma) + \mathbf{F}^{i-1}(\sigma). \qquad (18)$$

This equation is similar to equations describing dynamic systems (Palm, 1983). This is, of course, not very surprising, because we are regarding a non-steady-state (and therefore dynamic) system.

Due to matrix $\mathbf{A}$ several x_j^i-terms are coupled. A small computational error will accumulate and be amplified because of the iteration process that is necessary for calculating the solution at every time step. This is the well-known problem of stiffness. If we can find a diagonal matrix $\mathbf{D}$ instead of matrix $\mathbf{A}$, we will get a set of ordinary differential equations. Therefore we define matrices $\mathbf{A}$ and $\mathbf{Q}$, and vector $\mathbf{Y}$ such that the following holds:

$$\mathbf{AQ} = \mathbf{QD} \quad \text{and} \quad \mathbf{X} = \mathbf{QY} \Leftrightarrow \mathbf{Y} = \mathbf{Q}^{-1}\mathbf{X}. \quad (19)$$

Matrix $\mathbf{D}$ contains the eigenvalues of matrix $\mathbf{A}$. Matrix $\mathbf{Q}$ contains the eigenvectors of $\mathbf{A}$:

$$\mathbf{D} = \begin{bmatrix} d_1 & 0 & 0 & 0 \\ 0 & d_2 & 0 & 0 \\ 0 & 0 & d_3 & 0 \\ 0 & 0 & 0 & d_4 \end{bmatrix}$$

and

$$\mathbf{Q} = \begin{bmatrix} q_{11} & q_{12} & q_{13} & q_{14} \\ q_{21} & q_{22} & q_{23} & q_{24} \\ q_{31} & q_{32} & q_{33} & q_{34} \\ q_{41} & q_{42} & q_{43} & q_{44} \end{bmatrix}. \qquad (20)$$

Two negative and two positive eigenvalues were always found, due to the definition of the $\mathbf{A}$ matrix.

We chose to take d_1, $d_2 < 0$ and d_3, $d_4 > 0$. This is however not important, as long as the boundary conditions are correctly evaluated.

The eigenvector $\mathbf{Q}(i, j)$ belongs to the eigenvalue d_j $(i, j = 1, 2, 3, 4)$.

Substitution of eq. (19) in eq. (18) yields

$$\mathbf{Q} \cdot \frac{\mathrm{d}}{\mathrm{d}\sigma} \mathbf{Y}^i(\sigma) = \mathbf{A} \cdot \mathbf{Q} \cdot \mathbf{Y}^i(\sigma) + \mathbf{F}^{i-1}(\sigma) \qquad (21)$$

$$\Rightarrow \qquad \mathbf{Q} \cdot \frac{\mathrm{d}}{\mathrm{d}\sigma} \mathbf{Y}^i(\sigma) = \mathbf{Q} \cdot \mathbf{D} \cdot \mathbf{Y}^i(\sigma) + \mathbf{F}^{i-1}(\sigma) \qquad (22)$$

$$\Rightarrow \qquad \frac{\mathrm{d}}{\mathrm{d}\sigma} \mathbf{Y}^i(\sigma) = \mathbf{D} \cdot \mathbf{Y}^i(\sigma) + \tilde{\mathbf{F}}^{i-1}(\sigma)$$

with $\quad \tilde{\mathbf{F}}^{i-1}(\sigma) = \mathbf{Q}^{-1} \cdot \mathbf{F}^{i-1}(\sigma)$. $\qquad (23)$

Due to matrix $\mathbf{D}$ the y_j^i-terms are now decoupled. Equation (23) can be solved by standard procedures for the solution of inhomogeneous differential equations. First we define a homogenous solution $\mathbf{Y}_h^i(\sigma)$:

$$\mathbf{Y}_h^i(\sigma) = \begin{bmatrix} e^{d_1\sigma} & 0 & 0 & 0 \\ 0 & e^{d_2\sigma} & 0 & 0 \\ 0 & 0 & e^{d_3(\sigma-1)} & 0 \\ 0 & 0 & 0 & e^{d_4(\sigma-1)} \end{bmatrix}. \qquad (24)$$

The $(\sigma - 1)$ terms has been chosen to make sure that the solution can easily be calculated at $\sigma = 1$, as will be shown later.

The particular solution can be determined using the following equations:

$$\frac{\mathrm{d}}{\mathrm{d}\sigma} p_j(\sigma) = d_j \cdot p_j(\sigma) + \tilde{f}_j^{i-1}(\sigma) \qquad (j = 1, 2, 3, 4)$$

with $\quad p_1(0) = 0, \ p_2(0) = 0, \ p_3(1) = 0, \ p_4(1) = 0.$ $\quad (25)$

For the complete solution we get

$$\mathbf{Y}^i(\sigma) = \mathbf{c}^i \cdot \mathbf{Y}_h^i(\sigma) + \mathbf{P}^i(\sigma). \qquad (26)$$

Here vector $\mathbf{P}^i(\sigma)$ contains the $p_j^i(\sigma)$ terms defined in eq. (25). The constant vector $\mathbf{c}^i$ can be found by evaluating the boundary conditions. Writing eqs (8)–(11) in x_j^i-terms, we get

$$x_1^i(0) = c_f + \zeta_1 \cdot x_3^i(0) \text{ with } \zeta_1 = 1/(f_b \cdot Pe_b) \qquad (27)$$

$$x_2^i(0) = c_f + \zeta_2 \cdot x_4^i(0) \text{ with } \zeta_2 = 1/[(1-f_b)Pe_d] \qquad (28)$$

$$x_3^i(1) = 0 \qquad (29)$$

$$x_4^i(1) = 0. \qquad (30)$$

This leads to

$$[1 \quad 0 \quad -\zeta_1 \quad 0] \cdot \mathbf{X}^i(0) = c_f \qquad (31)$$

$$[0 \quad 1 \quad 0 \quad -\zeta_2] \cdot \mathbf{X}^i(0) = c_f \qquad (32)$$

$$[0 \quad 0 \quad 1 \quad 0] \cdot \mathbf{X}^i(1) = 0 \qquad (33)$$

$$[0 \quad 0 \quad 0 \quad 1] \cdot \mathbf{X}^i(1) = 0. \qquad (34)$$

Substitution of $\mathbf{X} = \mathbf{Q} \cdot \mathbf{Y}$ gives

$$[1 \ 0 \ -\zeta_1 \ 0] \cdot \mathbf{Q} \cdot \mathbf{Y}^i(0) = c_f, \text{ etc.}$$

Evaluating these equations with eq. (26) leads to

$$\mathbf{E} \cdot \mathbf{c}^i = \mathbf{g}^i \qquad (35)$$

with

$$\mathbf{E} = \begin{bmatrix} q_{11} - \zeta_1 q_{31} & q_{12} - \zeta_1 q_{32} & (q_{13} - \zeta_1 q_{33})e^{-d_3} & (q_{14} - \zeta_1 q_{34})e^{-d_4} \\ q_{21} - \zeta_2 q_{41} & q_{22} - \zeta_2 q_{42} & (q_{23} - \zeta_2 q_{43})e^{-d_3} & (q_{24} - \zeta_2 q_{44})e^{-d_4} \\ q_{31}e^{d_1} & q_{32}e^{d_2} & q_{33} & q_{34} \\ q_{41}e^{d_1} & q_{42}e^{d_2} & q_{43} & q_{44} \end{bmatrix} \qquad (36a)$$

and

$$\mathbf{g}^i = \begin{bmatrix} c_f - p_3^i(0) \cdot (q_{13} - \zeta_1 q_{33}) - p_4^i(0) \cdot (q_{14} - \zeta_1 q_{34}) \\ c_f - p_3^i(0) \cdot (q_{23} - \zeta_2 q_{43}) - p_4^i(0) \cdot (q_{24} - \zeta_2 q_{44}) \\ -p_1^i(1) \cdot q_{31} - p_2^i(1) \cdot q_{32} \\ -p_1^i(1) \cdot q_{41} - p_2^i(1) \cdot q_{42} \end{bmatrix}. \qquad (36b)$$

The following holds:

$$\mathbf{c}^i = \mathbf{E}^{-1} \cdot \mathbf{g}^i. \qquad (37)$$

Because the inverse matrix $\mathbf{E}^{-1}$ can introduce some computational inaccuracies (NAG, 1980), it was always checked whether the constant vector $\mathbf{c}^i$ calculated by eq. (37) fulfilled eq. (35). This was always the case.

For $p_j^i(\sigma)$ eq. (25) holds. In finding $p_3^i(\sigma)$ and $p_4^i(\sigma)$ the end conditions for these variables have to transformed into initial conditions. We have

$$\mathrm{d}p_j^i(\sigma)/\mathrm{d}\sigma = d_j^i p_j(\sigma) = \tilde{f}_j^{i-1}(\sigma) \quad \text{with} \quad p_j^i(1) = 0$$

$$(j = 3, 4) \qquad (38)$$

We now define

$$t_j^i(\sigma) = p_j^i(1 - \sigma) \quad (j = 3, 4). \qquad (39)$$

This leads to

$$\mathrm{d}t_j^i(\sigma)/\mathrm{d}\sigma = -\mathrm{d}p_j^i(1 - \sigma)/\mathrm{d}\sigma = -d_j \cdot p_j^i(1 - \sigma)$$
$$-\tilde{f}_j^{i-1}(1 - \sigma) \quad (j = 3, 4). \quad (40)$$

Therefore

$$\mathrm{d}t_j^i(\sigma)/\mathrm{d}\sigma = -d_j \cdot t_j^i(\sigma) - \tilde{f}_j^{i-1}(1 - \sigma)$$
$$\text{with } t_j^i(0) = 0 \quad (j = 3, 4). \quad (41)$$

The end condition is now transformed into an initial condition and computation is possible. When $t_j^i(\sigma)$ has been calculated, $p_j^i(\sigma)$ can be found by interchanging the values according to eq. (39).

In calculating $p_j^i(\sigma)$, $\tilde{f}_j^{i-1}(\sigma)$ has to be known. This means that an $\tilde{f}_j^{i-1}$ value has to be known at every possible σ. This is done by curve-fitting the concentration profile of the preceding time step $(i - 1)$ with a cubic-spline fit (Hayes, 1974). The integration routine can calculate every $\tilde{f}_j^{i-1}$ value at every desired σ value, and not only at the points specified by the user.

A semi-analytical solution of eq. (25) is also possible. Then a polynomial curve fit of the concentration profiles has to be substituted in the analytical solution. Of course this is only possible if the curve fit can describe the actual curve with high enough accuracy. To start with and for simplicity, we have used a numerical solution using the Gear method.

For calculational purposes (stability) the equations for $\mathbf{P}^i(\sigma)$ have been changed somewhat by eliminating $\Delta\vartheta$. By means of vector $\mathbf{F}^{i-1} \Delta\vartheta$ is introduced [eq. (17)]. Multiplying by $\Delta\vartheta$ leads to

$$\mathrm{d}\tilde{\mathbf{P}}^i(\sigma)/\mathrm{d}\sigma = \mathbf{D} \cdot \tilde{\mathbf{P}}^i(\sigma) + \tilde{\mathbf{R}}^{i-1}(\sigma) \qquad (42)$$

with

$$\tilde{\mathbf{P}}^i(\sigma) = \Delta\vartheta \cdot \mathbf{P}^i(\sigma) \text{ and } \tilde{\mathbf{R}}^{i-1}(\sigma) = \Delta\vartheta \cdot \tilde{\mathbf{F}}^{i-1}(\sigma). \qquad (43)$$

With vector $\tilde{\mathbf{R}}^{i-1} \Delta\vartheta$ is now eliminated. This does not change anything about the preceding.

The same derivations can of course be used when neglecting one or two of the axial dispersion coefficients E_b and/or E_d. The resulting matrices for $(E_b = 0, E_d \neq 0)$ and $(E_b = 0, E_d = 0)$ are given in Appendix A. It is furthermore stressed that with this method it is necessary for the parameters to be independent of height (except for the concentrations of course). Otherwise the decoupling with the matrices can not be performed.

ALGORITHM

Calculations were done with the NAG library (1980–1989). Computation can of course also be done with other libraries and if necessary routines can be written by the user himself.

All used routines will be given at every step. A summary of all the major steps is:

(1) Find $\mathbf{Q}$ and $\mathbf{D}$, such that $\mathbf{AQ} = \mathbf{QD}$ (eigenvalues and eigenvectors).
(2) Define $\mathbf{Y}^i(\sigma) = \mathbf{Q}^{-1} \cdot \mathbf{X}^i(\sigma)$, leading to $\mathrm{d}\mathbf{Y}^i(\sigma)/\mathrm{d}\sigma = \mathbf{D} \cdot \mathbf{Y}^i(\sigma) + \tilde{\mathbf{F}}^{i-1}(\sigma)$, with $\tilde{\mathbf{F}}^{i-1}(\sigma) = \mathbf{Q}^{-1} \cdot \mathbf{F}^{i-1}(\sigma)$.
(3) Compute $\mathbf{Y}^i(\sigma)$ from the homogeneous and particulate solution: $\mathbf{Y}^i(\sigma) = \mathbf{c}^i \cdot \mathbf{Y}_h^i(\sigma) + \mathbf{P}^i(\sigma)$, with $\mathbf{c}^i = \mathbf{E}^{-1} \mathbf{g}^i$.
(4) The final solution is found by back-transformation: $\mathbf{X}^i(\sigma) = \mathbf{Q} \cdot \mathbf{Y}^i(\sigma)$.

The accuracy of the calculation can be controlled in three ways. First of all, the integration routine [for $\tilde{\mathbf{P}}^i(\sigma)$] requires a tolerance. Secondly, the user can specify many or few σ points at which a solution is desired. Thirdly, the $\Delta\vartheta$ value has a direct control over matrix $\mathbf{A}$ and therefore also over matrices $\mathbf{Q}$ and $\mathbf{D}$.

A flow sheet is given in Fig. 2. Eigenvalues and eigenvectors are calculated with the NAG routine F02AGF, and inverse matrix with the routine F01AAF. A cubic-spline fit is done with E02BAF, and an evaluation of the fit is done with E02BBF. Furthermore we used the integration routine D02EBF (Gear method routine).
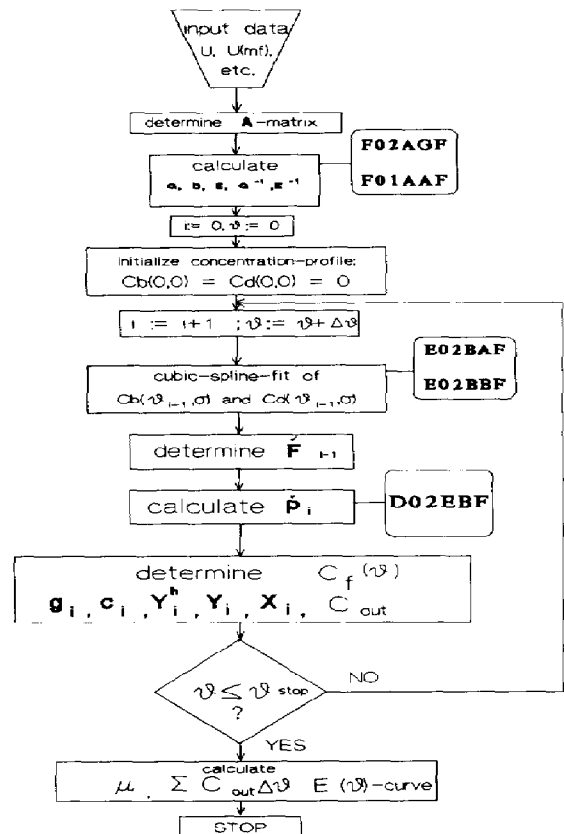

Fig. 2. Flow sheet of program.

Definition of feed and end conditions

For the RTD the injection pulse has been defined as a Dirac pulse:

$$C_f(t) = a_d \exp\left[-\pi^2 a_d^2 (t - t_{\text{step}})^2\right]. \qquad (44)$$

The t_{step} value has been introduced to make sure that the pulse is injected completely and gradually (numerically speaking). For the final RTD curve this t_{step} value has to be subtracted from the t values. The response on a Dirac pulse with t_{step} equal to zero will be known.

Making eq. (44) dimensionless yields

$$C_f(\vartheta) = a_d \exp\left[-\pi^2 a_d^2 (H\,\xi/U)^2 (\vartheta - \vartheta_{\text{step}})^2\right]. \qquad (45)$$

Because the surface under a Dirac pulse equals unity this leads to

$$\int_0^\infty C_f(\vartheta)\,\mathrm{d}\vartheta = 1/\tau = C_0 \qquad (46)$$

with τ being the average residence time, and C_0 the total amount of tracer gas injected.

The total amount of tracer gas entering the reactor has to leave the reactor (no reaction) and therefore

$$\int_0^\infty C_f(\vartheta)\,\mathrm{d}\vartheta = \int_0^\infty C_{\text{out}}(\vartheta)\,\mathrm{d}\vartheta = 1/\tau. \qquad (47)$$

Because C_0 equals $1/\tau$, this also leads to the condition that the surface under the $E(\vartheta)$ curve (which is the dimensionless response), equals unity:

$$\int_0^\infty C_{\text{out}}(\vartheta)\,\mathrm{d}\vartheta = 1/\tau = C_0 \Rightarrow \int_0^\infty \frac{C_{\text{out}}(\vartheta)}{C_0}\,\mathrm{d}\vartheta$$

$$= \int_0^\infty E(\vartheta)\,\mathrm{d}\vartheta = 1. \qquad (48)$$

We checked whether the calculations fulfilled these conditions by taking a summation value according to

$$\sum_0^{\vartheta_{\text{stop}}} C_{\text{out}}(\vartheta)\Delta\vartheta = 1/\tau = \frac{U}{H\xi}. \qquad (49)$$

The ϑ_{stop} value has always been taken large enough to acquire a constant summation value, implying that $\vartheta_{\text{stop}} \to \infty$.

Another check was performed by calculating the average residence time from the simulated curves. This value has to be equal to $\vartheta = 1$.

To fulfill eq. (44) numerically, we computed an a_d value according to

$$\text{minimize}\left\{\left[\sum_0^{\vartheta_{\text{stop}}} C_f(\vartheta)\Delta\vartheta\right] - (1/\tau)\right\}. \qquad (50)$$

RESULTS AND DISCUSSION

The program was written in FORTRAN and run on VAX/VMS. The CPU time was in the order of 1–5 min, depending upon matrix type, step sizes and tolerance used with the calculations. For all calculations the input parameters listed in Table 1 were used. As an example we used these values because

they are usually encountered in laboratory scale reactors. Fan and Fan (1979, 1980) for instance used the same order of values. They also showed that *Pe* could be taken independent of height. Computation is, of course, also possible with values that refer to commercial units.

We defined a relative error in the following way:

$$\varepsilon_{\text{rel}} = \frac{|\text{value calculated} - \text{value wanted}|}{|\text{value wanted}|} \cdot 100\%. \qquad (51)$$

Relative errors based on residence time and surface beneath the curve were calculated. The best $\Delta\vartheta$ and $\Delta\sigma$ values, as well as knots for the cubic-spline fit, were determined by taking those values that gave stable solutions with a small relative error. The boundaries for the integration routine were taken to be $\sigma = 0$ and $\sigma = 1$. All solutions were calculated with $\Delta\sigma = 0.01$ and $\Delta\vartheta = 0.01$. The step size in placing the knots was taken to be 0.02.

The tolerance in calculating $\tilde{p}_i(\sigma)$ was 10^{-5}. If necessary 10^{-7} was taken. This way, a maximum relative error of $\simeq 5\%$ was always found. Most calculations gave a relative error of 1–3%.

First of all a comparison was made between the finite-difference method (NAG routine D03PGF) and the decoupling method. Results for $Pe_b = 20$, $Pe_d = 20$ and $N_k = 2$ are shown in Fig. 3. This shows that both methods lead to the same result. The difference only occurs in the height of the top. The place and shape of the first peak, caused by the bubbles, are equal. Dense-phase gas leaves the reactor more slowly

Table 1. List of parameter values used in computation

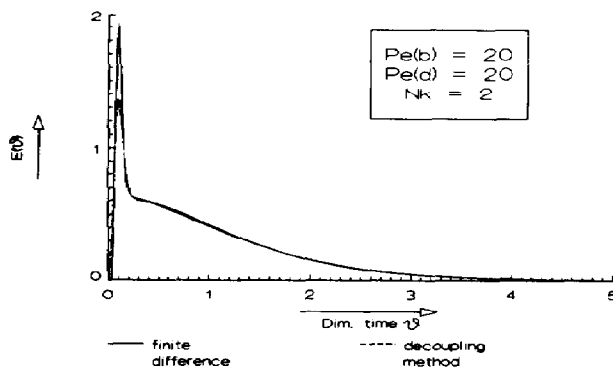| |
|---|
| $U = 0.1$ m/s |
| $U_{mf} = 0.01$ m/s |
| $\delta = 0.05$ |
| $\varepsilon_d = 0.40$ |
| $H = 1.0$ m |
| $\varphi = 1.0$ |

Fig. 3. Comparison of residence time distributions of finite-difference method and decoupling method.

and gradually, giving the tail. The shape and place of the tail are again the same for both methods.

Due to the stiffness the finite-difference method often gave erroneous answers, particularly at somewhat "low" Pe ($\leqslant 10$) and "high" N_k ($\geqslant 5$–10). The decoupling method always returned a stable solution with a relative error of less than 5%.

Computations were also made with the non-steady-state reaction system. The height concentration profile and resulting conversion were the same as for the steady-state reaction system, using the decoupling method and analytical solutions.

Various computations were made with different parameter values. Neglecting one or two Pe terms leads, in principle, to difference systems. This is because the resulting matrices are completely different. Yet comparable solutions were obtained, as is shown in Figs 4–10. This indicates the stability of the decoupling method.

All this shows that the decoupling method is a stable method leading to good results.

Figure 4 shows results for the (2×2) matrix, with $Pe_b \to \infty$, $Pe_d \to \infty$ and N_k as the parameter. At $N_k = 2$ gas exchange is relatively small and, because bubbles rise much more faster than the dense-phase gas, a peak occurs. When the gas exchange increases the curve maximum shifts more towards $\vartheta = 1$, because more gas is transported upwards in the relatively slow dense phase. If the exchange would get
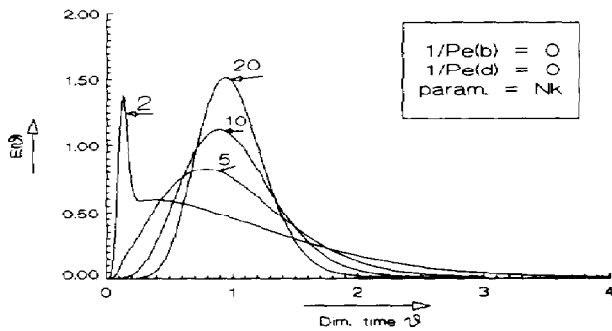

Fig. 6. Residence time distribution with fixed Pe_b and N_k and variable Pe_d [(3×3) matrix].

Fig. 7. Residence time distribution with fixed Pe_b and N_k and variable Pe_d [(3×3) matrix].

Fig. 4. Residence time distribution with fixed Pe_b and Pe_d and variable N_k [(2×2) matrix].

Fig. 8. Residence time distribution with fixed Pe_b and Pe_d and variable N_k [(4×4) matrix].
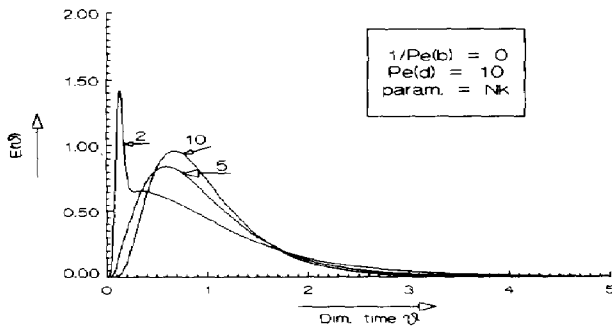

Fig. 5. Residence time distribution with fixed Pe_b and Pe_d and variable N_k [(3×3) matrix].
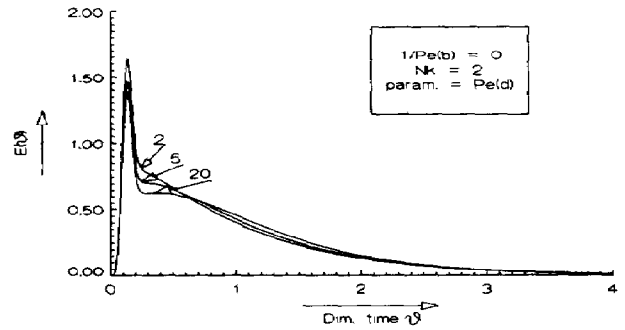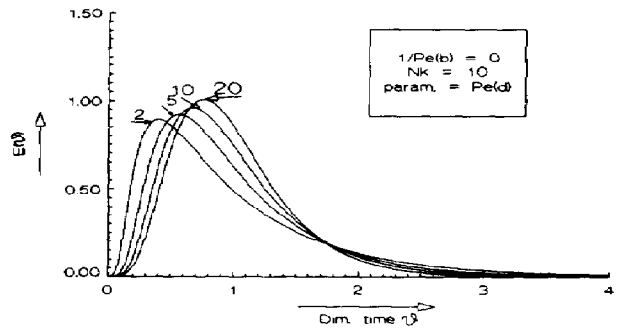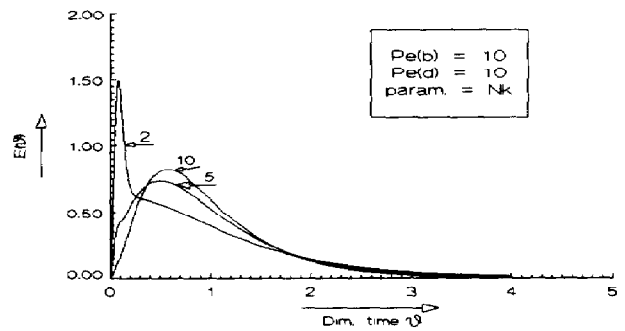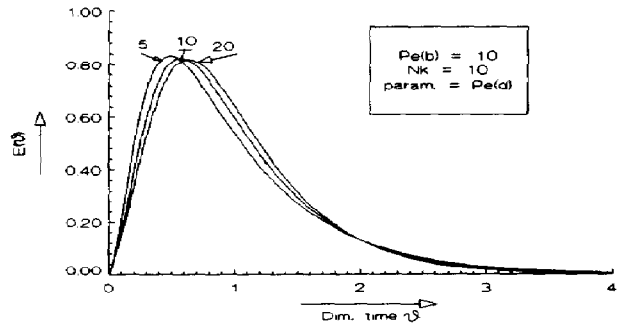

Fig. 9. Residence time distribution with fixed Pe_b and N_k and variable Pe_d [(4×4) matrix].
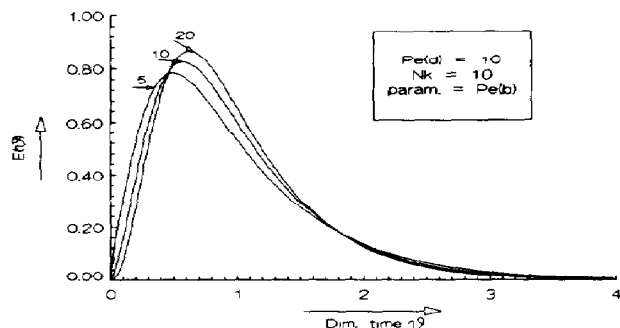
Fig. 10. Residence time distribution with fixed N_k and Pe_d and variable Pe_b [(4 × 4) matrix].

infinitely great, equilibrium would be reached and the gas would rise in plug flow. Therefore there will be a Gaussian peak at $\vartheta = 1$ for large N_k. The average residence time of the total gas is described with eq. (3c) and of the bubble phase with eq. (3a). This shows that $\tau_b/\tau \simeq \delta/\xi \cong 0.12$ (with $\delta = 0.05$ and $\varepsilon_d = 0.4$). This value is indeed found from Fig. 4.

Comparable results were obtained with the (3 × 3) matrix, with $Pe_b \to \infty$, $Pe_d = 10$ and N_k as the parameter (Fig. 5). As can be seen from Figs 4 and 5, the influence of N_k is sufficient to obtain a reliable N_k value from RTD measurements.

The influence of Pe_d is shown in Fig. 6. At $N_k = 2$ the influence is not that obvious because most gas flows through the reactor in the bubble phase. With $N_k = 10$ (Fig. 7), the influence is much more obvious, due to the higher exchange to the dense phase. At low Pe_d the dense phase approaches an ideal mixed system. Therefore, the top of the curve will shift towards $\vartheta = 0$. Similar results for the (4 × 4) matrix are shown in the Figs 8–10.

CONCLUDING REMARKS

We deduced equations from the bubble dispersion model that can be used for all types of powders.

A finite difference was taken in the time variable instead of in the space variable. After rewriting these equations, using rather elementary mathematics, the equations were decoupled. Comparable computations were performed with the standard Crank–Nicholson technique and the decoupling method. This showed that both methods gave the same results if calculation was possible with the Crank–Nicholson technique.

The advantages of the decoupling method are that it is straightforward, mathematically not very complex, and leads to good and stable solutions. Of course it should be possible to use the decoupling method for other non-steady- and steady-state systems. In principle it can be used for a system of many equations, as long as it is possible to calculate the eigenvectors, eigenvalues and inverse matrices with high enough accuracy. An example can be found in Tuin (1989).

To start with we have taken a grid with uniform spacing. It will, of course, be economically more efficient if a non-uniform spacing is used. For simplicity

we have not yet done that. This does however not affect the decoupling method itself. A semi-analytical solution for eq. (25), describing the particular part, might also give some improvement. This, however, is only the case if an accurate polynomial curve fit is possible. This means that many fluctuations in the curve should give problems. More research is needed in these areas.

RTD analysis for all types of powders is now possible, if sufficient data on the hydrodynamics are available. In our future research, hydrodynamics will be measured and RTD measurements will be performed.

NOTATION

a	specific bubble surface, m^2/m^3
a_d	coefficient in Dirac pulse [eq. (44)]
A	cross-sectional area of reactor, m^2
C_b	gas concentration in bubble phase
C_d	gas concentration in dense phase
C_0	total amount of gas injected
C_f	feed concentration
C_{out}	average concentration of gas leaving the reactor
d_j	eigenvalues of matrix A
E_b	Eddy dispersion coefficient for bubble phase, m^2/s
E_d	Eddy disperion coefficient for dense phase, m^2/s
$E(\vartheta)$	dimensionless response (C_{out}/C_0).
f_b	fraction of gas in the bubble phase
f_j	elements vector $\bar{F}^{i-1}$
h	differential bed height, m
H	total bed height, m
i	subscript
j	subscript
K_e	mass transfer coefficient based on total gas volume, s^{-1}
k_m	reaction constant based on catalyst mass [eq. (2)], kg/(m^3 s)
k_g	mass transfer coefficient, m/s
N_k	number mass transfer units
N_r	number of reaction units
Pe_b	Peclet number for bubble phase
Pe_d	Peclet number for dense phase
p_j	elements of particulate vector $\mathbf{P}^i(\sigma)$
t_j	transformation elements for p_j elements [eq. (39)]
U	superficial velocity, m/s
u_b	bubble velocity, m/s
u_d	dense-phase gas velocity, m/s
U_{mf}	minimum fluidization velocity, m/s

Greek letters

β	gas parameter for bubble phase [eqs (4) and (12)]

γ	gas parameter for dense phase [eqs (5) and (12)]
δ	bubble hold up
ε_d	dense-phase porosity
ε_{rel}	relative error [eq. (51)]
ζ	parameter for boundary conditions [eqs (27) and (28)]
μ	average residence time calculated by program simulation
φ	through flow factor for dense phase
ρ_p	particle density, kg/m^3
ϑ	dimensionless time (t/τ)
ϑ_{step}	dimensionless time step for Dirac pulse [eq. (45)]
ϑ_{stop}	dimensionless time at which computations are stopped
$\Delta\vartheta$	step size for dimensionless time
σ	dimensionless height (h/H)
$\Delta\sigma$	step size for dimensionless height
τ	average residence time based on total amount of gas in reactor, s
τ_b	average residence time based on gas in bubble phase, s
τ_d	average residence time based on gas in dense phase, s
ξ	total gas fraction in reactor $[\delta + (1 - \delta)\varepsilon_d]$

Matrices/vectors

A	matrix containing original parameters [eqs (17) and (18)]
c	constant vector for homogeneous solution [eq. (26)]
D	diagonal matrix containing the eigenvalues of **A** [eqs (19) and (20)]
E	matrix obtained by evaluating the boundary conditions [eq. (35)]
F	vector containing concentrations from time step $i - 1$ [eq. (18)]
F̃	"decoupled" vector **F** $(= \mathbf{Q}^{-1}\mathbf{F})$ [eq. (23)]
g	vector obtained evaluating the feed and boundary conditions [eq. (37)]
P	matrix for particulate solution [eq. (26)]
P̃	matrix **P** with extracted $\Delta\vartheta$ values [eq. (42)]
Q	matrix containing the eigenvectors of **A** [eq. (19)]
R̃	vector **F** with extracted $\Delta\vartheta$ values [eq. (42)]
X	original vector containing bubble and dense phase concentrations [eqs (17) and (18)]
Y	"decoupled" vector **X** $(= \mathbf{Q}^{-1}\mathbf{X})$ [eq. (19)]
Y$_h$	homogeneous part of solution differential equation [eq. (24)]

REFERENCES

Bauer, W., 1980, Einfluss der Gasverteilerkonstruktion auf Stoffaustausch- und Reactionsverhalten flacher Wirbelschichten. Ph.D. thesis, Universität Erlangen.

Dry, R. J. and Judd, M. R., 1985, Fluidized beds of fine, dense powders. Scale-up and reactor modeling. *Powder Technol.* **43**, 41–53.

Eigenberger, G. and Butt, J. B., 1976, A modified Crank–Nicholson technique with equidistant space steps. *Chem. Engng Sci.* **3**, 681–691.

Fan, L. T. and Fan, L.-S., 1979, Simulation of catalytic fluidized bed reactors by a transient axial dispersion model with invariant physical properties and nonlinear chemical reactions. *Chem. Engng Sci.* **34**, 171–179.

Fan, L.-S. and Fan, L. T., 1980, Transient and steady state characteristics of a gaseous reactant in catalytic fluidized bed reactions. *A.I.Ch.E. J.* **26**, 139.

Geldart, D., 1973, Types of fluidization. *Powder Technol.* **7**, 285.

Grace, J. R. and Clift, R., 1974, On the two-phase theory of fluidization. *Chem. Engng Sci.* **29**, 327–334.

Hayes, J. G., 1974, Numerical methods for curve and surface fitting. *Bull. Inst. math. Applic.* **10**, 144.

Hlavacek, V. and van Rompay, P., 1981, Current problems of multiplicity, stability and sensitivity of states in chemically reacting systems. *Chem. Engng Sci.* **36**, 1587–1597.

NAG library, 1980, Chapter 3 from Introduction of F01-routines, Mark 8.

Numerical Algorithm Group Limited, 1980–1989, NAG FORTRAN Library, Oxford.

Palm, W. J., 1983, Advanced matrix methods for dynamic system analysis, in *Modeling Analysis and Control of Dynamic Systems*, Chap. 9, p. 583. John Wiley, New York.

Tuin, B. J. W., 1989, Extraction of heavy metals from contaminated clay soils, p. 166. Ph.D. thesis, Eindhoven University of Technology.

van Deemter, J. J., 1961, Mixing and contacting in gas–solid fluidized beds. *Chem. Engng Sci.* **13**, 143–154.

van Lare, C. E. J., Piepers, H. W. and Thoenes, D., 1990, Scaling and particle size optimization of mass transfer in gas fluidized beds. *Chem. Engng Sci.* **45**, 2211–2217.

van Loon, P., 1987, Continuous decoupling transformations for linear boundary value problems. Ph.D. thesis, Eindhoven University of Technology.

van Swaaij, W. P. M. and Zuiderweg, F. J., 1972, Investigation of ozone decomposition in fluidized beds on the basis of a two-phase model. *Chem. React. Engng Proc. 5th Eur. Symp.*, B9–25.

Villadsen, J. V. and Stewart, W. E., 1967, Solution of boundary-value problems by orthogonal collocation. *Chem. Engng Sci.* **22**, 1483–1501.

Werther, J., 1978, Mathematische modellierung von Wirbelschichtreaktoren. *Chemie-Ingr-Tech.* **50**, 850.

APPENDIX A

Matrix definition when neglecting Pe_b *term*
Original equations:

$$\frac{\partial C_b}{\partial \vartheta} + \beta \frac{\partial C_b}{\partial \sigma} + N_k \frac{\xi}{\delta}(C_b - C_d) = 0 \qquad (A1)$$

$$\frac{\partial C_d}{\partial \vartheta} + \gamma \frac{\partial C_d}{\partial \sigma} + \frac{N_k \xi}{(1-\delta)\varepsilon_d}(C_d - C_b)$$

$$- \frac{1}{Pe_d}\frac{\xi}{(1-\delta)\varepsilon_d}\frac{\partial^2 C_d}{\partial \sigma^2} + N_r \frac{\xi}{(1-\delta)\varepsilon_d} C_d = 0 \quad (A2)$$

with boundary conditions

$$C_b(0, \sigma) = 0 \qquad (A3)$$

$$C_d(0, \sigma) = 0 \qquad (A4)$$

$$C_b(\vartheta, 0) = C_f(\vartheta) \quad (\vartheta > 0) \qquad (A5)$$

$$C_d(\vartheta, 0) = C_f(\vartheta) + \frac{1}{(1-f_b)Pe_d}\frac{\partial C_d}{\partial \sigma}\bigg]_{\sigma = 0} \quad (\vartheta > 0) \qquad (A6)$$

$$\frac{\partial C_d}{\partial \sigma}\bigg]_{\sigma = 1} = 0 \qquad (A7)$$

Euler approximation of time variable:

$$\frac{\partial C_{b,i}}{\partial \sigma} = -\frac{N_k}{f_b}(C_{b,i} - C_{d,i}) - \frac{C_{b,i} - C_{b,i-1}}{\Delta\vartheta}\frac{1}{\beta} \qquad (A8)$$

$$\frac{\partial^2 C_{d,i}}{\partial \sigma^2} = (1 - f_b) Pe_d \frac{\partial C_{d,i}}{\partial \sigma} + N_k \cdot Pe_d \cdot (C_{d,i} - C_{b,i})$$

$$+ N_r \cdot Pe_d \cdot C_{d,i} + \frac{C_{d,i} - C_{d,i-1}}{\Delta \vartheta} \frac{Pe_d (1 - \delta) \varepsilon_d}{\xi} . \quad \text{(A9)}$$

Taking $N_r = 0$ (no reaction) leads to

$$\frac{\mathrm{d}}{\mathrm{d}\sigma} \begin{bmatrix} C_{b,i} \\ C_{d,i} \\ \partial C_{d,i}/\partial \sigma \end{bmatrix} = \begin{bmatrix} -(N_k/f_b + 1/(\beta \cdot \Delta \vartheta)) & N_k/f_b & 0 \\ 0 & 0 & 1 \\ -N_k \cdot Pe_d & Pe_d(N_k + (1-\delta)\varepsilon_d/(\xi \cdot \Delta \vartheta)) & (1-f_b)Pe_d \end{bmatrix} \begin{bmatrix} C_{b,i} \\ C_{d,i} \\ \partial C_{d,i}/\partial \sigma \end{bmatrix}$$

$$+ \begin{bmatrix} \dfrac{1}{\beta \Delta \vartheta} C_{b,i-1} \\ 0 \\ -\dfrac{Pe_d(1-\delta)\varepsilon_d}{\xi \Delta \vartheta} C_{d,i-1} \end{bmatrix} . \qquad \text{(A10)}$$

Matrix definition when neglecting Pe_b *and* Pe_d *terms*
Original equations:

$$\frac{\partial C_b}{\partial \vartheta} + \beta \frac{\partial C_b}{\partial \sigma} + N_k \frac{\xi}{\delta} (C_b - C_d) = 0 \qquad \text{(A11)}$$

$$\frac{\partial C_d}{\partial \vartheta} + \gamma \frac{\partial C_d}{\partial \sigma} + \frac{N_k \xi}{(1-\delta)\varepsilon_d} (C_d - C_b)$$

$$+ N_r \frac{\xi}{(1-\delta)\varepsilon_d} C_d = 0 \quad \text{(A12)}$$

with boundary condition

$$C_b(0, \sigma) = 0 \qquad \text{(A13)}$$

$$C_d(0, \sigma) = 0 \qquad \text{(A14)}$$

$$C_b(\vartheta, 0) = C_f(\vartheta) \quad (\vartheta > 0) \qquad \text{(A15)}$$

$$C_d(\vartheta, 0) = C_f(\vartheta) \quad (\vartheta > 0). \qquad \text{(A16)}$$

Taking an Euler approximation in the time variable and $N_r = 0$:

$$\frac{\partial C_{b,i}}{\partial \sigma} = -\frac{N_k}{f_b} (C_{b,i} - C_{d,i}) - \frac{C_{b,i} - C_{b,i-1}}{\Delta \vartheta} \frac{1}{\beta} \quad \text{(A17)}$$

$$\frac{\partial C_{d,i}}{\partial \sigma} = -\frac{N_k}{(1-f_b)} (C_{d,i} - C_{b,i}) - \frac{C_{d,i} - C_{d,i-1}}{\Delta \vartheta} \frac{1}{\gamma}. \quad \text{(A18)}$$

Writing in matrix form yields

$$\frac{\mathrm{d}}{\mathrm{d}\sigma} \begin{bmatrix} C_{b,i} \\ C_{d,i} \end{bmatrix} = \begin{bmatrix} -(N_k/f_b + 1/(\beta \cdot \Delta \vartheta)) & N_k/f_b \\ N_k/(1-f_b) & -(N_k/(1-f_b) + 1/(\gamma \cdot \Delta \vartheta)) \end{bmatrix} \begin{bmatrix} C_{b,i} \\ C_{d,i} \end{bmatrix} + \begin{bmatrix} \dfrac{1}{\beta \cdot \Delta \vartheta} C_{b,i-1} \\ \dfrac{1}{\gamma \cdot \Delta \vartheta} C_{d,i-1} \end{bmatrix} . \quad \text{(A19)}$$